EUROPEAN ORGANIZATION FOR NUCLEAR RESEARCH (CERN)

CERN-EP-2016-315
LHCb-PAPER-2016-041
2 April 2017

arXiv:1701.01871v2 [hep-ex] 1 Jun 2017

Measurement of *CP* asymmetries in $D^{\pm} \to \eta'\pi^{\pm}$ and $D_s^{\pm} \to \eta'\pi^{\pm}$ decays

The LHCb collaboration[†]

Abstract

A search for *CP* violation in $D^{\pm} \to \eta'\pi^{\pm}$ and $D_s^{\pm} \to \eta'\pi^{\pm}$ decays is performed using proton-proton collision data, corresponding to an integrated luminosity of $3\,\text{fb}^{-1}$, recorded by the LHCb experiment at centre-of-mass energies of 7 and 8 TeV. The measured *CP*-violating charge asymmetries are $\mathcal{A}_{CP}(D^{\pm} \to \eta'\pi^{\pm}) = (-0.61 \pm 0.72 \pm 0.53 \pm 0.12)\%$ and $\mathcal{A}_{CP}(D_s^{\pm} \to \eta'\pi^{\pm}) = (-0.82 \pm 0.36 \pm 0.22 \pm 0.27)\%$, where the first uncertainties are statistical, the second systematic, and the third are the uncertainties on the $\mathcal{A}_{CP}(D^{\pm} \to K_S^0\pi^{\pm})$ and $\mathcal{A}_{CP}(D_s^{\pm} \to \phi\pi^{\pm})$ measurements used for calibration. The results represent the most precise measurements of these asymmetries to date.

Published in Phys. Lett. B 771 (2017) 21-30

© CERN on behalf of the LHCb collaboration, licence CC-BY-4.0.

[†]Authors are listed at the end of this Letter.

1 Introduction

The decays of charmed mesons offer a unique opportunity for the experimental investigation of hitherto unobserved *CP* violation in the up-type quark sector. The Standard Model (SM) predicts *CP* violation to occur in the charm sector, albeit at a level of $\mathcal{O}(10^{-3})$ at leading order in $1/m_c$, compatible with the lack of evidence in current measurements. Larger values are possible if new sources of *CP* violation beyond the SM exist. The study of charm systems is a unique tool to probe sources of *CP* violation that affect only the dynamics of up-type quarks [1].

In order for non-zero *CP* asymmetries to be observable in a process, two or more interfering amplitudes with different *CP*-odd and *CP*-even phases are needed. In the SM, no direct *CP* violation can therefore emerge at leading order in Cabibbo-favoured charm decays, which are mediated by a single weak amplitude, while small *CP* asymmetries are expected in singly-Cabibbo-suppressed decays [2] due to the interference of colour-allowed tree-level amplitudes with loop- (penguin) and colour-suppressed tree-level amplitudes. Since these asymmetries may be enhanced by nonperturbative effects [3], theoretical interpretations of experimental results require the analysis of several channels with similar sensitivity. In particular, the study of charm decays to pseudoscalar mesons tests flavour topology [4] and SU(3) predictions, and may constrain amplitudes through triangle relations or shed light on sources of SU(3) flavour symmetry breaking [5, 6, 7]. To date, the most precise measurements of *CP* asymmetries in singly-Cabibbo-suppressed two-body charm decays have been performed in $D^0 \to K^+K^-$ and $D^0 \to \pi^+\pi^-$ decays by the LHCb collaboration [8, 9], and have shown no evidence for *CP* violation. Among the other charm decays to two pseudoscalar mesons with significant branching fractions, thus far $D^\pm \to \eta'\pi^\pm$ and $D_s^\pm \to \eta'\pi^\pm$ have been studied only in e^+e^- collisions [10, 11] due to the experimental difficulty of reconstructing $\eta^{(\prime)}$ mesons in hadron collisions. The most recent studies of these decays at the Belle and CLEO experiments yielded a *CP* asymmetry of $(-0.12 \pm 1.12 \pm 0.17)\%$ [11] for the singly-Cabibbo-suppressed $D^\pm \to \eta'\pi^\pm$ decay and $(-2.2 \pm 2.2 \pm 0.6)\%$ [10] for the Cabibbo-favoured $D_s^\pm \to \eta'\pi^\pm$ decay, respectively.

In this Letter the first analysis of $D^\pm_{(s)} \to \eta'\pi^\pm$ decays at a hadron collider is presented, using proton-proton (pp) collision data corresponding to an integrated luminosity of approximately $3\,\text{fb}^{-1}$, collected by the LHCb experiment. This allows for the large charm yields available at the LHC to be exploited, resulting in the most precise measurement of *CP* asymmetries in these decays to date.

2 Method

The *CP* asymmetries $\mathcal{A}_{CP}$ are determined from the measured (raw) asymmetries

$$\mathcal{A}_{\text{raw}}(D^\pm_{(s)} \to f^\pm) = \frac{N(D^+_{(s)} \to f^+) - N(D^-_{(s)} \to f^-)}{N(D^+_{(s)} \to f^+) + N(D^-_{(s)} \to f^-)}, \tag{1}$$

where N denotes the observed yield for the decay to a given charged final state $f^\pm$. The measured asymmetries include additional contributions other than $\mathcal{A}_{CP}(D^\pm_{(s)} \to f^\pm)$. For small asymmetries, it is possible to approximate to first order

$$\mathcal{A}_{\text{raw}} \approx \mathcal{A}_{CP} + \mathcal{A}_{\text{P}} + \mathcal{A}_{\text{D}}, \tag{2}$$

where $\mathcal{A}_{\rm P}$ is the asymmetry in the production of $D^{\pm}_{(s)}$ mesons in high-energy pp collisions in the LHCb acceptance, and $\mathcal{A}_{\rm D}$ arises from the difference in detection efficiencies between positively and negatively charged hadrons.

These effects are studied using control decay modes for which $\mathcal{A}_{CP}$ is known precisely. The control decays, which have similar decay topologies as the signal decays, are the Cabibbo-favoured $D^{\pm} \to K^0_{\rm S}\pi^{\pm}$ and $D^{\pm}_s \to \phi\pi^{\pm}$ decays for $D^{\pm} \to \eta'\pi^{\pm}$ and $D^{\pm}_s \to \eta'\pi^{\pm}$, respectively. The CP asymmetries in these control decays have been measured at the 10^{-3} level by the Belle and D0 collaborations [12, 13].

The differences between the CP asymmetries measured in the $D^{\pm}_{(s)} \to \eta'\pi^{\pm}$ decays and in the corresponding control channels are defined as

$$\begin{aligned}
\Delta\mathcal{A}_{CP}(D^{\pm} \to \eta'\pi^{\pm}) &\equiv \mathcal{A}_{CP}(D^{\pm} \to \eta'\pi^{\pm}) - \mathcal{A}_{CP}(D^{\pm} \to K^0_{\rm S}\pi^{\pm}) \\
&= \mathcal{A}_{\rm raw}(D^{\pm} \to \eta'\pi^{\pm}) - \mathcal{A}_{\rm raw}(D^{\pm} \to K^0_{\rm S}\pi^{\pm}) + \mathcal{A}(\overline{K}^0 - K^0), \\
\Delta\mathcal{A}_{CP}(D^{\pm}_s \to \eta'\pi^{\pm}) &\equiv \mathcal{A}_{CP}(D^{\pm}_s \to \eta'\pi^{\pm}) - \mathcal{A}_{CP}(D^{\pm}_s \to \phi\pi^{\pm}) \\
&= \mathcal{A}_{\rm raw}(D^{\pm}_s \to \eta'\pi^{\pm}) - \mathcal{A}_{\rm raw}(D^{\pm}_s \to \phi\pi^{\pm}).
\end{aligned} \tag{3}$$

These equations assume that the kinematic distributions of the pion and of the $D_{(s)}$ meson are similar in the signal and control channels, so that detection and production asymmetries largely cancel in the difference. The uncertainty associated to this assumption is discussed in Sec. 5. The $\mathcal{A}(\overline{K}^0 - K^0)$ term in Eq. 3 represents the kaon asymmetry in $D^{\pm} \to K^0_{\rm S}\pi^{\pm}$ decays, which arises from regeneration and from mixing and CP violation in the $\overline{K}^0 - K^0$ system. This contribution is estimated using simulations, as described in Ref. [9], to be $(-0.08 \pm 0.01)\%$. The CP asymmetry in the singly-Cabibbo-suppressed $D^{\pm} \to \eta'\pi^{\pm}$ decay is therefore given by

$$\mathcal{A}_{CP}(D^{\pm} \to \eta'\pi^{\pm}) \approx \Delta\mathcal{A}_{CP}(D^{\pm} \to \eta'\pi^{\pm}) + \mathcal{A}_{CP}(D^{\pm} \to K^0_{\rm S}\pi^{\pm}). \tag{4}$$

Similarly, the CP asymmetry for the Cabibbo-favoured $D^{\pm}_s \to \eta'\pi^{\pm}$ decay is approximated as

$$\mathcal{A}_{CP}(D^{\pm}_s \to \eta'\pi^{\pm}) \approx \Delta\mathcal{A}_{CP}(D^{\pm}_s \to \eta'\pi^{\pm}) + \mathcal{A}_{CP}(D^{\pm}_s \to \phi\pi^{\pm}). \tag{5}$$

3 Detector

The LHCb detector [14, 15] is a single-arm forward spectrometer covering the pseudorapidity range $2 < \eta < 5$, designed for the study of particles containing b or c quarks. The detector includes a high-precision tracking system consisting of a silicon-strip vertex detector surrounding the pp interaction region, a large-area silicon-strip detector located upstream of a dipole magnet with a bending power of about 4 Tm, and three stations of silicon-strip detectors and straw drift tubes placed downstream of the magnet. The polarity of the dipole magnet is reversed periodically throughout data taking. The configuration with the magnetic field vertically upwards (downwards) bends positively (negatively) charged particles in the horizontal plane towards the centre of the LHC. The tracking system provides a measurement of momentum, p, of charged particles with a relative uncertainty that varies from 0.5% at low momentum to 1.0% at 200 GeV/c. The minimum distance of a track to a primary vertex (PV), the impact parameter (IP), is measured with a resolution of $(15 + 29/p_{\rm T})\,\mu$m, where $p_{\rm T}$ is the component of the momentum transverse to the beam, in GeV/c. Different types of charged hadrons are distinguished

using information from two ring-imaging Cherenkov detectors. Photons, electrons and hadrons are identified by a calorimeter system consisting of scintillating-pad and preshower detectors, an electromagnetic calorimeter and a hadronic calorimeter. Muons are identified by a system composed of alternating layers of iron and multiwire proportional chambers. The online event selection is performed by a trigger, which consists of a hardware stage, based on information from the calorimeter and muon systems, followed by a software stage, which applies a full event reconstruction. At the hardware trigger stage, events are required to have a muon with high $p_{\rm T}$ or a hadron, photon or electron with high transverse-energy deposit in the calorimeters.

In the simulation, pp collisions are generated using Pythia 6.4 [16] with a specific LHCb configuration [17]. Decays of hadronic particles are described by EvtGen [18], in which final-state radiation is generated using Photos [19]. The interaction of the generated particles with the detector, and its response, are implemented using the Geant4 toolkit [20] as described in Ref. [21].

4 Reconstruction and sample composition

The data correspond to an integrated luminosity of approximately $3\,\text{fb}^{-1}$ recorded in pp collisions at centre-of-mass energies of $\sqrt{s} = 7\,\text{TeV}$ ($1\,\text{fb}^{-1}$) and $8\,\text{TeV}$ ($2\,\text{fb}^{-1}$). Approximately 50% of the data were collected in each configuration of magnet polarity. The $\mathcal{A}_{\rm raw}$ measurements are performed separately for the two field polarities and the two centre-of-mass energies.

The signal $D^{\pm}_{(s)} \to \eta'\pi^{\pm}$ candidates, as well as control $D^{\pm} \to K^0_{\rm S}\pi^{\pm}$ and $D^{\pm}_s \to \phi\pi^{\pm}$ candidates, are reconstructed through the intermediate resonance decays $\eta' \to \pi^+\pi^-\gamma$, $K^0_{\rm S} \to \pi^+\pi^-$, and $\phi \to K^+K^-$. The sample is divided into three mutually exclusive subsamples according to the fulfilled hardware trigger requirements. The first subsample, T1, consists of events for which the trigger decision is based on the transverse energy deposited in the hadronic calorimeter by a charged particle from the decay of the η', $K^0_{\rm S}$, or ϕ meson. The second subsample, T2, consists of the subset of the remaining events for which a particle other than the decay products of the $D^{\pm}_{(s)}$ candidate is associated with a high transverse-energy deposit in the hadronic calorimeter. The third subsample, T3, consists of the events accepted because of a high transverse-energy deposit in the electromagnetic calorimeter or a high-$p_{\rm T}$ muon, not associated with the $D^{\pm}_{(s)}$ decay and not included in the other subsamples. The hardware trigger selections do not rely on information associated with the same-charge pion from the $D^{\pm}_{(s)}$ decay.

One or more of the charged decay products from the η', $K^0_{\rm S}$, or ϕ meson is required to activate the first stage of the software trigger, which selects a sample with enhanced heavy-flavour content by requiring the presence of a large-IP charged particle with $p_{\rm T} > 1.6$ GeV/c ($p_{\rm T} > 1.7$ GeV/c) in the $8\,\text{TeV}$ ($7\,\text{TeV}$) data. In the second stage of the software trigger, each selected event is required to contain at least one combination of three tracks that meet loose requirements on the IP of the final-state particles and on the invariant mass of the charged decay products.

For the $D^{\pm}_{(s)} \to \eta'\pi^{\pm}$ channels, the η' candidates are reconstructed by combining pairs of oppositely charged particles with a photon of $p_{\rm T} > 1$ GeV/c. The η' charged decay products must not be identified as kaons by the particle identification system [15], and must be displaced from the PV. Photon candidates are reconstructed from clusters of

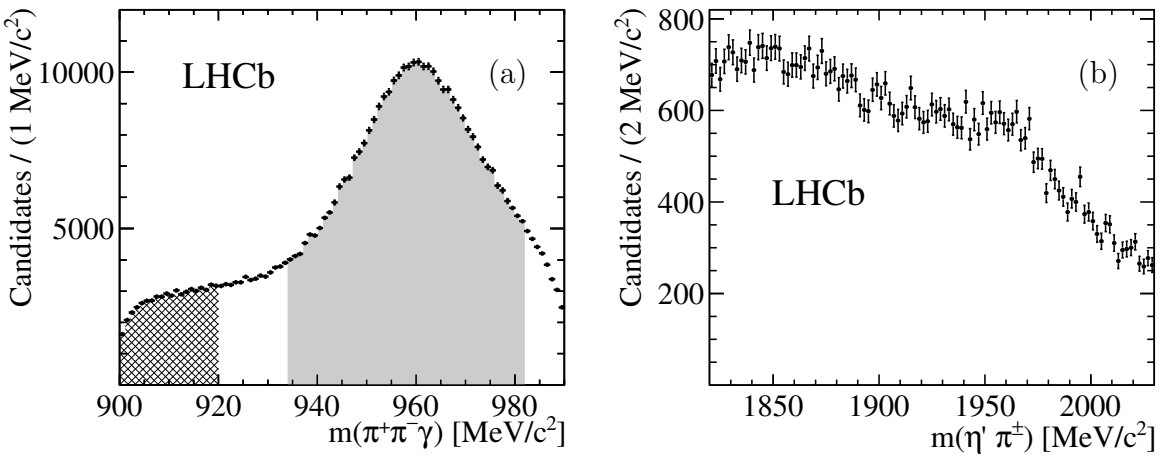


Figure 1: Distribution of (a) $m(\pi^+\pi^-\gamma)$ for $D^\pm_{(s)} \to \eta'\pi^\pm$ candidates. The grey solid area represents the signal region, while the black hatched area represents the $m(\pi^+\pi^-\gamma)$ sideband. Distribution of (b) $m(\eta'\pi^\pm)$ for $D^\pm_{(s)} \to \eta'\pi^\pm$ candidates in the $m(\pi^+\pi^-\gamma)$ sideband.

energy deposits in the electromagnetic calorimeter. The absence of tracks pointing to the energy-cluster barycentre is used to distinguish neutral from charged particles. For high-$p_{\rm T}$ photons a multivariate algorithm based on the shape parameters of the cluster is used to reject $\pi^0 \to \gamma\gamma$ background in which the two photons are reconstructed as a single cluster [15]. To maximize sensitivity to $\mathcal{A}_{\rm raw}(D^\pm_{(s)} \to \eta'\pi^\pm)$, the three-particle mass is required to satisfy $0.934 < m(\pi^+\pi^-\gamma) < 0.982$ GeV/c^2, as shown in Fig. 1(a) by the light-shaded region.

The $K^0_{\rm S}$ candidates are formed from a pair of non-prompt, oppositely charged high-momentum particles reconstructed in the vertex detector. A good-quality vertex fit and sufficient separation from the PV are required for the decay vertex of the $K^0_{\rm S}$ candidate. The $\pi^+\pi^-$ mass is required to lie in the range $0.4626 < m(\pi^+\pi^-) < 0.5326$ GeV/c^2.

To reconstruct ϕ candidates, two oppositely charged, large-IP particles, classified as kaons by the particle identification system [15], are combined. The K^+K^- mass is required to be within ± 20 MeV/c^2 of the known ϕ mass [22].

Selected η', $K^0_{\rm S}$, and ϕ candidates are combined with a third non-prompt charged pion (bachelor particle) to form a $D^\pm_{(s)}$ candidate. The selection criteria for the bachelor pion are chosen to be as similar as possible between signal and control samples. To suppress background contributions from $D^\pm_{(s)} \to X\ell^\pm\nu$ and $D^\pm_{(s)} \to XK^\pm$ decays, with $X = \eta'$, ϕ, or $K^0_{\rm S}$, the bachelor particle must be identified as a pion rather than as an electron, muon or kaon. The lepton veto removes more than 95% of the electrons and muons and 9% of the pions, and the kaon veto rejects about 95% of the kaons while retaining 90% of all pions [15]. Fiducial requirements are imposed to exclude kinematic regions where reconstruction and particle identification of the bachelor pion suffer from large charge-dependent asymmetries [23].

Candidate $D^\pm_{(s)}$ mesons are required to have $p_{\rm T} > 2$ GeV/c in all decay modes, and mass in the range $1.82 < m(\eta'\pi^\pm) < 2.03$ GeV/c^2 for the signal $D^\pm_{(s)} \to \eta'\pi^\pm$ decays and $1.80 < m(K^0_{\rm S}\pi^\pm) < 2.03$ GeV/c^2 ($1.80 < m(\phi\pi^\pm) < 2.03$ GeV/c^2) for the $D^\pm \to K^0_{\rm S}\pi^\pm$ ($D^\pm_{(s)} \to \phi\pi^\pm$) control mode. To calculate the $D^\pm_{(s)}$ mass [24], the η' candidate mass is

constrained to its known value [22], without placing constraints on the origin of the $D^{\pm}_{(s)}$ meson. The charged decay products of the reconstructed $D^{\pm}_{(s)}$ candidates are required to match one of the three-track combinations that activated the second stage of the software trigger. The scalar sum of the transverse momenta of charged decay products must exceed 2.8 GeV/c for all decay modes. In events with multiple $D^{\pm}_{(s)}$ candidates only one randomly selected candidate is kept. This procedure removes less than 2% of the original candidates.

A combinatorial background contribution is present in all decay modes. Background from partially reconstructed $D^{\pm}_{s} \to \eta'\rho^{\pm}$ decays is suppressed by requiring $m(\eta'\pi^{\pm}) > 1.82$ GeV/c^2. Background from $D^{\pm}_{(s)} \to \pi^{\mp}\pi^{\pm}\pi^{\pm}$ decays, paired with a random photon, is suppressed by requiring the invariant mass of the three charged hadrons to be less than 1.80 GeV/c^2. A contribution from $D^{\pm}_{(s)} \to \phi\pi^{\pm}$ decays, with $\phi \to \pi^{+}\pi^{-}\pi^{0}$ (denoted below as $D^{\pm}_{(s)} \to \phi_{3\pi}\pi^{\pm}$), is also present, where one of the photons in the $\pi^0 \to \gamma\gamma$ decay is not reconstructed or the two photons are reconstructed as a single cluster.

Background from $D^{\pm}_{s} \to K^{0}_{\rm S}K^{\pm}$ and $D^{\pm}_{s} \to K^{0}_{\rm S}\pi^{\pm}\pi^{0}$ decays ($D^{\pm}_{s} \to \phi\pi^{\pm}\pi^{0}$ and non-resonant $D^{\pm}_{s} \to K^{+}K^{-}\pi^{\pm}$ decays), where the bachelor kaon is misidentified as a pion or the π^0 is not reconstructed, contributes negligibly to the $D^{\pm} \to K^{0}_{\rm S}\pi^{\pm}$ ($D^{\pm}_{s} \to \phi\pi^{\pm}$) candidate mass spectrum.

The $D^{\pm}_{(s)} \to \eta'\pi^{\pm}$ candidates originating from the decays of b hadrons are suppressed by requiring a good quality of the $D^{\pm}_{(s)}$ vertex fit, performed with the origin of the $D^{\pm}_{(s)}$ constrained to the associated PV but without a constraint on the η' candidate mass. Non-prompt $D^{\pm}_{s} \to \phi\pi^{\pm}$ and $D^{\pm} \to K^{0}_{\rm S}\pi^{\pm}$ candidates are rejected by requiring a small difference between the quality of the fit of the PV formed with and without the tracks assigned to the reconstructed $D^{\pm}_{(s)}$ candidate.

5 Determination of the asymmetries

For each final state, the data are divided into twelve mutually exclusive subsamples, according to the two pp centre-of-mass energies, two magnet polarities, and three hardware trigger selections. Since detection asymmetries depend on the kinematic properties of the process under study, $D^{\pm}_{(s)}$ candidates in each subsample are divided into 3×3 bins of transverse momentum and pseudorapidity of the bachelor pion. The bin edges in $p_{\rm T}$ are defined as 0.5, 1.5, 3.0, and 20.0 GeV/c, and the bin edges in η are defined as 2.0, 2.8, 3.2, and 5.0. While the kinematic distributions of the bachelor pion for the signal and $D^{\pm}_{s} \to \phi\pi^{\pm}$ control decays are in good agreement, the average bachelor-pion $p_{\rm T}$ (η) is 30% lower (5% higher) in the $D^{\pm} \to K^{0}_{\rm S}\pi^{\pm}$ control channel. The binning reduces the effect of the discrepancies between the bachelor-pion kinematic distributions for signal and control decays, thus improving the suppression of $\mathcal{A}_{\rm D}$ in the differences of raw asymmetries. For each of the twelve subsamples, the raw CP asymmetries of the $D^{\pm}_{(s)} \to \eta'\pi^{\pm}$ signal channels are determined with a maximum likelihood fit to the unbinned $\eta'\pi$ invariant mass distribution, performed simultaneously for positively and negatively charged $D^{\pm}_{(s)}$ candidates, and for the nine $p_{\rm T} - \eta$ bins.

The fit model comprises two signal components for the $D^{\pm}$ and $D^{\pm}_{s}$ resonances, a combinatorial background component, and two peaking components accounting for background from $D^{\pm}_{(s)} \to \phi_{3\pi}\pi^{\pm}$ decays. The signal components are modelled by Johnson

S_U distributions [25]:

$$f(x;\mu,\sigma,\delta,\gamma) \propto \left[1+\left(\frac{x-\mu}{\sigma}\right)^2\right]^{-\frac{1}{2}} \exp\left\{-\frac{1}{2}\left[\gamma+\delta\sinh^{-1}\left(\frac{x-\mu}{\sigma}\right)\right]^2\right\}. \quad (6)$$

The parameters μ and σ, which govern the mean and width of each distribution, are fitted independently for $D^\pm$ and $D_s^\pm$, and can vary with the charge and pseudorapidity of the bachelor pion. The remaining two parameters, δ and γ, characterising the tails of the Johnson S_U distributions, are common between the two signal components and are required to be the same across all $p_{\rm T}-\eta$ bins, but can vary with the charge of the bachelor pion. The combinatorial background is parametrised by a fourth-order polynomial, whose parameters can vary independently for positive and negative charges and for different bins in the bachelor-pion pseudorapidity. The parameters of the background model, for each charge and each bin in pseudorapidity of the bachelor pion, are Gaussian-constrained to the results of fits of the same functional form to the corresponding $m(\eta'\pi^\pm)$ distributions from the $m(\pi^+\pi^-\gamma)$ sideband (Fig. 1(b)). The $D^\pm_{(s)} \to \phi_{3\pi}\pi^\pm$ background components are described by empirical functions [26] derived from simulated events. The yields and charge asymmetries of signal and combinatorial components in each $p_{\rm T}-\eta$ bin, and the total yields of the $D^\pm_{(s)} \to \phi_{3\pi}\pi^\pm$ contributions are free parameters in the fit. For the $D^\pm_{(s)} \to \phi_{3\pi}\pi^\pm$ components, the raw *CP* asymmetries and the fraction of the total yields in each $p_{\rm T}-\eta$ bin are determined from $D^\pm_{(s)} \to \phi\pi^\pm$ control decays, with $\phi \to K^+K^-$. The model well reproduces the charge-integrated $m(\eta'\pi^\pm)$ distributions in all $p_{\rm T}$ bins. To estimate the goodness of fit, in each of the twelve subsamples the χ^2 of the fitted model is calculated for the binned $m(\eta'\pi^\pm)$ distribution in all $p_{\rm T}-\eta$ bins. The p-value is greater than 5% in all cases. The results of the fit to the $\eta'\pi$ mass distribution for $D^\pm_{(s)} \to \eta'\pi^\pm$ candidates are shown in Fig. 2. The signal yields, combined over all kinematic bins, pp centre-of-mass energies, and hardware trigger selections, are $N(D^\pm \to \eta'\pi^\pm) = (62.7 \pm 0.4) \times 10^3$ and $N(D_s^\pm \to \eta'\pi^\pm) = (152.2 \pm 0.5) \times 10^3$, respectively.

Due to the high purity of the control samples, the raw *CP* asymmetries for the $D_s^\pm \to \phi\pi^\pm$ and $D^\pm \to K^0_{\rm S}\pi^\pm$ decay modes are extracted by counting the numbers of positively and negatively charged candidates in the signal mass range and subtracting the corresponding numbers in the sidebands, shown in Fig. 3. For the $D^\pm \to K^0_{\rm S}\pi^\pm$ decay, the sidebands are defined as $1.800-1.835\,{\rm GeV}/c^2$ and $1.905-1.940\,{\rm GeV}/c^2$, and the signal range as $1.835-1.905\,{\rm GeV}/c^2$. For the $D_s^\pm \to \phi\pi^\pm$ channel the sidebands are defined as $1.910-1.935\,{\rm GeV}/c^2$ and $2.005-2.030\,{\rm GeV}/c^2$, and the signal range as $1.935-2.005\,{\rm GeV}/c^2$. The event yields determined in the $D_s^\pm \to \phi\pi^\pm$ sidebands are scaled by a factor 1.4 to account for the different widths of the sideband and signal ranges. Background from $D_s^\pm \to K^0_{\rm S}K^\pm$, $D_s^\pm \to K^0_{\rm S}\pi^\pm\pi^0$, $D_s^\pm \to \phi\pi^\pm\pi^0$, and non-resonant $D_s^\pm \to K^+K^-\pi^\pm$ decays is neglected. The effect of the small fraction of $D^\pm_{(s)}$ signal leaking into the sidebands, which may depend on the charge, p_T and pseudorapidity of the bachelor pion, is considered as a source of systematic uncertainty.

For each subsample, the differences of raw asymmetries for signal and associated control channels are calculated in each $p_{\rm T}-\eta$ bin. The weighted averages of the results obtained in the nine bins are then evaluated, taking into account the covariance matrix V, calculated as the sum of the covariance matrices for the results of the $D^\pm_{(s)} \to \eta'\pi^\pm$ fit and of the sideband subtraction for control decays. The weights are $w_i = \sum_k V^{-1}_{ik} / \left(\sum_j \sum_k V^{-1}_{jk}\right)$,

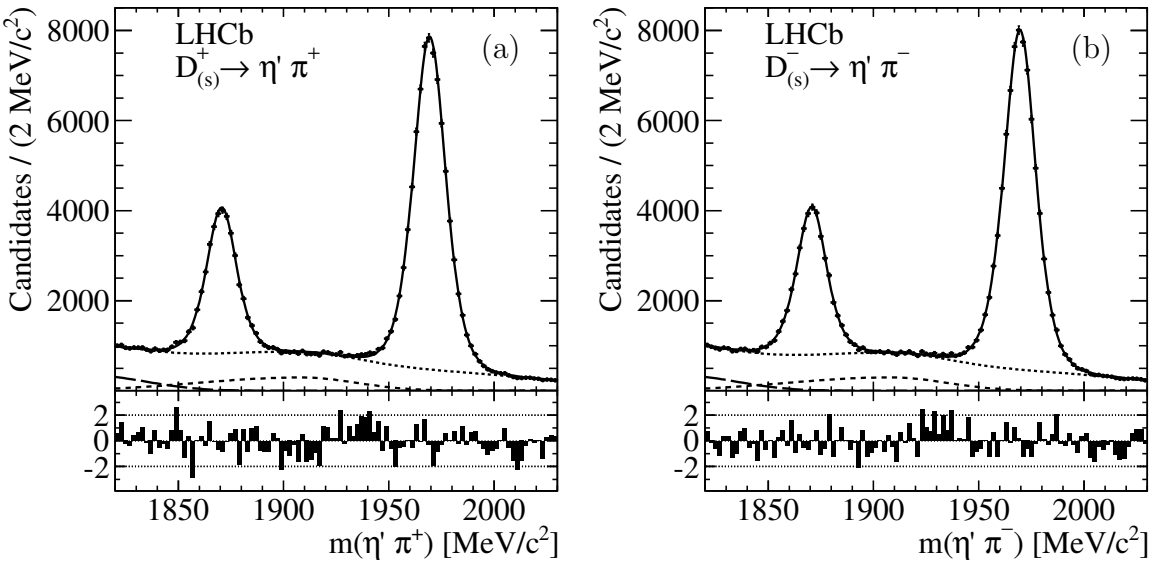


Figure 2: Mass distribution of $\eta'\pi^\pm$ candidates, combined over all kinematic bins, pp centre-of-mass energies, and hardware trigger selections, for (a) positively and (b) negatively charged $D^\pm_{(s)}$ candidates. Points with errors represent data, while the curves represent the fitted model (solid), the $D^\pm_s \to \phi_{3\pi}\pi^\pm$ (dashed) and $D^\pm \to \phi_{3\pi}\pi^\pm$ (long-dashed) components, and the sum of all background contributions (dotted), including combinatorial background. Residuals divided by the corresponding uncertainty are shown under each plot.

where i, j, and k run over the $p_{\rm T} - \eta$ bins. The resulting $\Delta\mathcal{A}_{CP}$ values are averaged with equal weights over the two magnet polarities. Detection asymmetries that differ between the signal and control decays are suppressed in this average. The results for the signal channels are shown in Fig. 4. Finally, the inverse-variance weighted average of the $\Delta\mathcal{A}_{CP}$ values obtained for the two pp centre-of-mass energies and the three hardware trigger selections is calculated. No significant charge asymmetry is observed for the combinatorial background component in any of the subsamples. The inverse-variance weighted average of $\mathcal{A}_{\rm raw}$ for the combinatorial background is $(0.92 \pm 0.72)\%$, where the error is statistical only.

6 Systematic uncertainties

The contributions to the systematic uncertainty on the inverse-variance weighted $\Delta\mathcal{A}_{CP}$ average are described below and summarised in Table 1. The overall systematic uncertainties are obtained by adding the individual contributions in quadrature.

The selection of signal and control sample candidates removes the majority of background from non-prompt $D^\pm_{(s)}$ mesons, originating from the decay of a b hadron. The remaining secondary $D^\pm_{(s)}$ mesons may introduce a bias in the measured CP asymmetries due to a difference in the production asymmetries for b hadrons and $D^\pm_{(s)}$ mesons. This bias might not cancel in the difference of measured asymmetries for signal and control channels, due to differences in the final-state reconstruction. In order to investigate this bias, the $D^\pm_{(s)}$ production asymmetries in $D^\pm_{(s)} \to \eta'\pi^\pm$ decays are modified using $\mathcal{A}'_{\rm P} = (\mathcal{A}_{\rm P} + f\mathcal{A}^b_{\rm P})/(1+f)$, where f is the fraction of secondary $D^\pm_{(s)}$ candidates in a

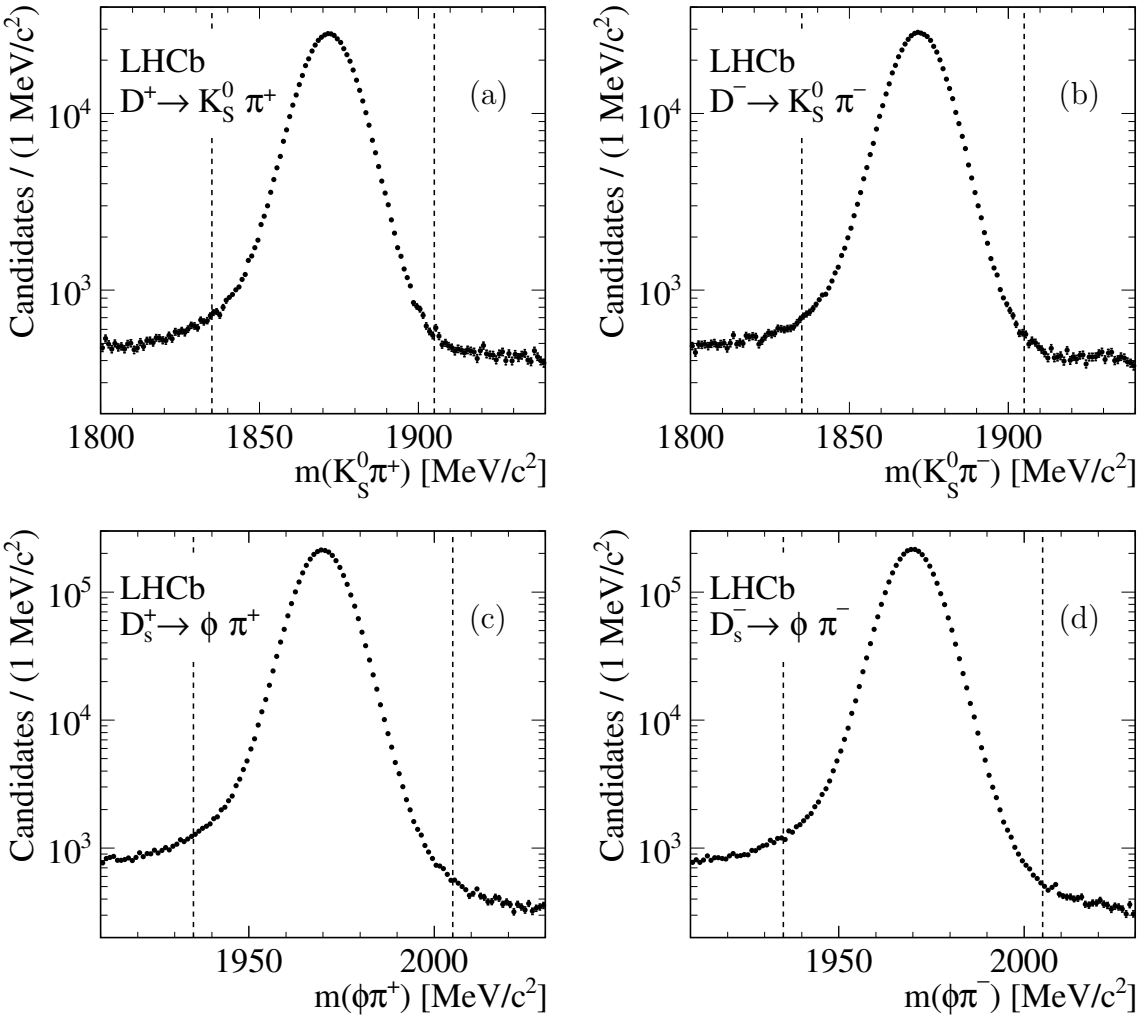


Figure 3: Top: $K^0_S\pi^\pm$ mass distribution for (a) positively and (b) negatively charged $D^\pm$ candidates. Bottom: $\phi\pi^\pm$ mass distribution for (c) positively and (d) negatively charged $D^\pm_s$ candidates. The signal regions are enclosed within the vertical dashed lines. The mass distributions are combined over all kinematic bins, *pp* centre-of-mass energies, and hardware trigger selections.

particular decay channel and $\mathcal{A}^b_{\rm P}$ is the corresponding b-hadron production asymmetry. The fraction f is estimated from the measured cross-sections for inclusive production of $D^\pm$, $D^\pm_s$, and b hadrons [27, 28], the inclusive branching fractions $\mathcal{B}(b \to D^\pm X)$ and $\mathcal{B}(b \to D^\pm_s X)$ [22], and the efficiencies calculated from simulation. The resulting values of f are below 6%. The b-hadron production asymmetry $\mathcal{A}^b_{\rm P}$ is taken from existing measurements for $B^\pm$, $B^0_{(s)}$, and Λ^0_b hadrons [29, 30, 31, 32, 33]. Under the assumption that the bias due to $\mathcal{A}^b_{\rm P}$ does not cancel in the difference of measured asymmetries for signal and control channels, the systematic uncertainty on $\Delta\mathcal{A}_{CP}$ is evaluated by recalculating the *CP* asymmetries using $\mathcal{A}'_{\rm P}$ for the signal decay modes and $\mathcal{A}_{\rm P}$ for the control samples.

Potential trigger biases are studied using $D^\pm_{(s)} \to \phi\pi^\pm$ decays, with $\phi \to K^+K^-$. The *CP* asymmetries measured in the subsamples defined by the T2 and T3 trigger selections are compared to the asymmetries from the T1 subsample, which is based on charge-

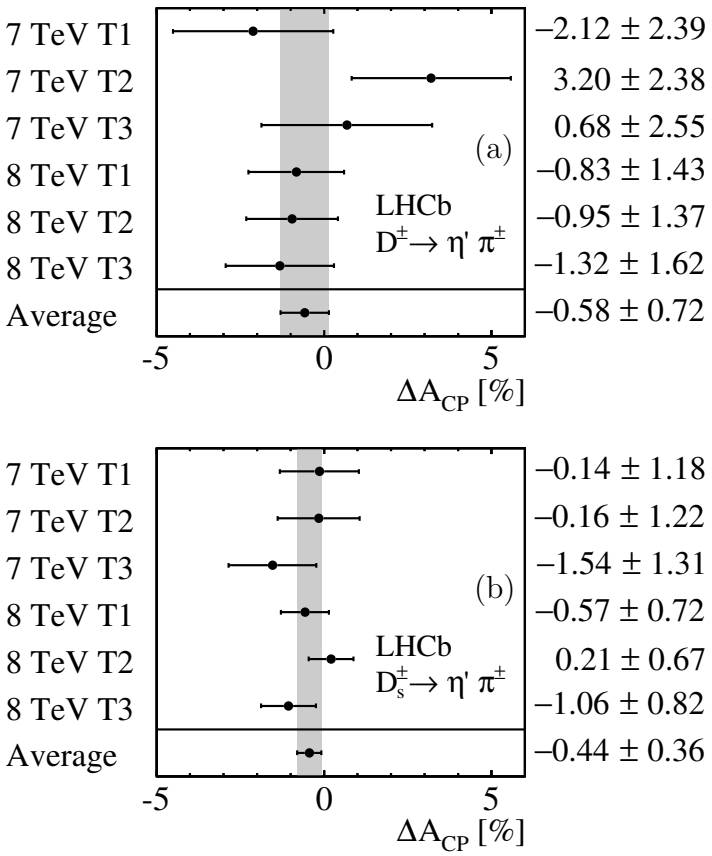


Figure 4: $\Delta\mathcal{A}_{CP}$ results for (a) $D^{\pm} \to \eta'\pi^{\pm}$ and (b) $D_s^{\pm} \to \eta'\pi^{\pm}$ decays, as a function of pp centre-of-mass energy and trigger selection. Uncertainties are statistical only. A shaded band representing the 68.3% confidence intervals obtained from the weighted average over all the samples is shown to guide the eye.

symmetric combinations of tracks. No statistically significant discrepancy is observed,

Table 1: Systematic uncertainties (absolute values in %) on $\Delta\mathcal{A}_{CP}$. The total systematic uncertainty is the sum in quadrature of the individual contributions.

Source	$\delta[\Delta\mathcal{A}_{CP}(D^{\pm})]$	$\delta[\Delta\mathcal{A}_{CP}(D_s^{\pm})]$
Non-prompt charm	0.03	0.03
Trigger	0.09	0.09
Background model	0.50	0.19
Fit procedure	0.08	0.04
Sideband subtraction	0.03	0.02
K^0 asymmetry	0.08	–
$\pi^{\pm}$ detection asymmetry	0.06	0.01
$D^{\pm}_{(s)}$ production asymmetry	0.07	0.02
Total	0.53	0.22

and the statistical uncertainty of the difference is assigned as a systematic uncertainty. This systematic uncertainty accounts for residual trigger-induced biases in the difference of measured asymmetries for signal and control channels.

Different background parametrizations can change the ratio of signal and background and affect the observed asymmetry. The nominal model is modified by replacing, for all subsamples, the fourth-order polynomial with other empirically chosen functions, a second-order polynomial or an ARGUS function [34]. Different fit configurations are tested, in which the background parameters are fixed according to the results of a fit to the $m(\pi^+\pi^-\gamma)$ sideband, or in which the $D^\pm_{(s)} \to \phi_{3\pi}\pi^\pm$ background fractions are varied. The maximum deviations from the results of the nominal fit, observed with any of the alternative models providing a reasonable fit to the data, are assigned as systematic uncertainties. This represents the largest contribution to the systematic uncertainties in both channels. This estimate is in agreement with an independent assessment, based on the increased statistical uncertainties on $\mathcal{A}_{\rm raw}$ when the constraints on the background parameters are removed from the nominal model.

The fitting procedure is validated with several pseudoexperiments using events simulated according to the fit model, varying the $\mathcal{A}_{\rm raw}$ value used in generation. The sum in quadrature of the bias and of its statistical uncertainty is taken as a systematic uncertainty.

A systematic uncertainty is introduced for the background contributions neglected in the measurement of the raw asymmetries for the $D^\pm \to K^0_{\rm S}\pi^\pm$ and $D^\pm_s \to \phi\pi^\pm$ control decays, and for the neglected fraction of $D^\pm_{(s)}$ signal leaking into the sidebands. The effect of non-resonant $D^\pm_s \to K^+K^-\pi^\pm$ contributions to the $D^\pm_s \to \phi\pi^\pm$ control sample is evaluated by observing the variation of $\Delta\mathcal{A}_{CP}(D^\pm_s \to \eta'\pi^\pm)$ when the K^+K^- mass is required to be within ± 10 MeV/c^2 (instead of ± 20 MeV/c^2) of the known ϕ mass. The systematic uncertainty due to $D^\pm_s \to K^0_{\rm S}K^\pm$, $D^\pm_s \to K^0_{\rm S}\pi^\pm\pi^0$, and $D^\pm_s \to \phi\pi^\pm\pi^0$ is calculated from the estimated fraction of background events, assuming a negligible CP violation and using the production asymmetries in LHCb acceptance as an input. The difference of raw asymmetries in $\Delta\mathcal{A}_{CP}(D^\pm \to \eta'\pi^\pm)$ is corrected for the K^0 asymmetry [9] and an associated systematic uncertainty equal to the applied correction is included.

The potential discrepancy in the bachelor pion kinematic distribution within each $p_{\rm T} - \eta$ bin between signal and control samples, associated to the finite number of bins, might result in an incomplete cancellation of detection asymmetries. The discrepancy in $\Delta\mathcal{A}_{CP}$ with respect to the nominal binning, resulting from using no kinematic binning, is assigned as a systematic uncertainty.

The $D^\pm_{(s)}$ production asymmetry may show a dependence on $p_{\rm T}$ and η of the charm meson. Therefore, the cancellation of production effects in $\Delta\mathcal{A}_{CP}$ may be partial, since $D^\pm_{(s)}$ kinematic distributions are different for signal and control channels. To estimate this effect, in each bin of the bachelor-pion kinematic distribution, the $D^\pm \to K^0_{\rm S}\pi^\pm$ and $D^\pm_s \to \phi\pi^\pm$ candidates are given a weight depending on either the $p_{\rm T}$ or the η value of the $D^\pm_{(s)}$ meson, to reproduce the $D^\pm_{(s)}$ kinematic distribution of signal candidates. The effect on $\Delta\mathcal{A}_{CP}$ is assigned as a systematic uncertainty.

The $\Delta\mathcal{A}_{CP}$ results are stable when the requirements on the bachelor-pion particle identification and track quality are tightened, and when the constraints on the parameters of the combinatorial background component are removed from the fit to $D^\pm_{(s)} \to \eta'\pi^\pm$ candidates. The stability of $\Delta\mathcal{A}_{CP}$ is also investigated as a function of beam energy and hardware trigger decision. No significant dependence is observed, as shown in Fig. 4.

7 Results and summary

Using pp collision data collected by the LHCb experiment at centre-of-mass energies of 7 and 8 TeV, the differences in CP asymmetries between $D^\pm \to \eta'\pi^\pm$ and $D^\pm \to K^0_S\pi^\pm$ decays, and between $D^\pm_s \to \eta'\pi^\pm$ and $D^\pm_s \to \phi\pi^\pm$ decays, are measured to be

$$\Delta\mathcal{A}_{CP}(D^\pm \to \eta'\pi^\pm) = (-0.58 \pm 0.72 \pm 0.53)\%,$$
$$\Delta\mathcal{A}_{CP}(D^\pm_s \to \eta'\pi^\pm) = (-0.44 \pm 0.36 \pm 0.22)\%.$$

In all cases, the first uncertainties are statistical and the second are systematic.

Using the previously measured values of the CP asymmetries in control decays, $\mathcal{A}_{CP}(D^\pm \to K^0_S\pi^\pm) = (-0.024 \pm 0.094 \pm 0.067)\%$ [12] and $\mathcal{A}_{CP}(D^\pm_s \to \phi\pi^\pm) = (-0.38 \pm 0.26 \pm 0.08)\%$ [13], the individual CP asymmetries are found to be

$$\mathcal{A}_{CP}(D^\pm \to \eta'\pi^\pm) = (-0.61 \pm 0.72 \pm 0.53 \pm 0.12)\%,$$
$$\mathcal{A}_{CP}(D^\pm_s \to \eta'\pi^\pm) = (-0.82 \pm 0.36 \pm 0.22 \pm 0.27)\%,$$

where the last contribution to the uncertainty comes from the $\mathcal{A}_{CP}(D^\pm \to K^0_S\pi^\pm)$ and $\mathcal{A}_{CP}(D^\pm_s \to \phi\pi^\pm)$ measurements.

The measured values show no evidence of CP violation, and are consistent with SM expectations [35, 36, 37] and with previous results obtained in e^+e^- collisions [10, 11]. The results represent the most precise measurements of these quantities to date.

Acknowledgements

We express our gratitude to our colleagues in the CERN accelerator departments for the excellent performance of the LHC. We thank the technical and administrative staff at the LHCb institutes. We acknowledge support from CERN and from the national agencies: CAPES, CNPq, FAPERJ and FINEP (Brazil); NSFC (China); CNRS/IN2P3 (France); BMBF, DFG and MPG (Germany); INFN (Italy); FOM and NWO (The Netherlands); MNiSW and NCN (Poland); MEN/IFA (Romania); MinES and FASO (Russia); MinECo (Spain); SNSF and SER (Switzerland); NASU (Ukraine); STFC (United Kingdom); NSF (USA). We acknowledge the computing resources that are provided by CERN, IN2P3 (France), KIT and DESY (Germany), INFN (Italy), SURF (The Netherlands), PIC (Spain), GridPP (United Kingdom), RRCKI and Yandex LLC (Russia), CSCS (Switzerland), IFIN-HH (Romania), CBPF (Brazil), PL-GRID (Poland) and OSC (USA). We are indebted to the communities behind the multiple open source software packages on which we depend. Individual groups or members have received support from AvH Foundation (Germany), EPLANET, Marie Skłodowska-Curie Actions and ERC (European Union), Conseil Général de Haute-Savoie, Labex ENIGMASS and OCEVU, Région Auvergne (France), RFBR and Yandex LLC (Russia), GVA, XuntaGal and GENCAT (Spain), Herchel Smith Fund, The Royal Society, Royal Commission for the Exhibition of 1851 and the Leverhulme Trust (United Kingdom).

References

[1] Y. Grossman, A. L. Kagan, and Y. Nir, *New physics and CP violation in singly Cabibbo suppressed D decays*, Phys. Rev. **D75** (2007) 036008, arXiv:hep-ph/0609178.

[2] F. Buccella, M. Lusignoli, and A. Pugliese, *Charm nonleptonic decays and final state interactions*, Phys. Lett. **B379** (1996) 249, arXiv:hep-ph/9601343.

[3] M. Golden and B. Grinstein, *Enhanced CP violations in hadronic charm decays*, Phys. Lett. **B222** (1989) 501.

[4] L.-L. Chau, *Quark mixing in weak interactions*, Phys. Rept. **95** (1983) 1.

[5] I. Hinchliffe and T. A. Kaeding, *Nonleptonic two-body decays of D mesons in broken SU(3)*, Phys. Rev. **D54** (1996) 914, arXiv:hep-ph/9502275.

[6] B. Bhattacharya and J. L. Rosner, *Charmed meson decays to two pseudoscalars*, Phys. Rev. **D81** (2010) 014026, arXiv:0911.2812.

[7] H.-Y. Cheng and C.-W. Chiang, *SU(3) symmetry breaking and CP violation in $D \to PP$ decays*, Phys. Rev. **D86** (2012) 014014, arXiv:1205.0580.

[8] LHCb collaboration, R. Aaij *et al.*, *Measurement of the difference of time-integrated CP asymmetries in $D^0 \to K^-K^+$ and $D^0 \to \pi^-\pi^+$ decays*, Phys. Rev. Lett. **116** (2016) 191601, arXiv:1602.03160.

[9] LHCb collaboration, R. Aaij *et al.*, *Measurement of CP asymmetry in $D^0 \to K^-K^+$ and $D^0 \to \pi^-\pi^+$ decays*, JHEP **07** (2014) 041, arXiv:1405.2797.

[10] CLEO collaboration, P. U. E. Onyisi *et al.*, *Improved measurement of absolute hadronic branching fractions of the D_s^+ meson*, Phys. Rev. **D88** (2013) 032009, arXiv:1306.5363.

[11] Belle collaboration, E. Won *et al.*, *Observation of $D^+ \to K^+\eta^{(\prime)}$ and search for CP violation in $D^+ \to \pi^+\eta^{(\prime)}$ decays*, Phys. Rev. Lett. **107** (2011) 221801, arXiv:1107.0553.

[12] Belle collaboration, B. R. Ko *et al.*, *Evidence for CP violation in the decay $D^+ \to K^0_S\pi^+$*, Phys. Rev. Lett. **109** (2012) 021601, Erratum ibid. **109** (2012) 119903, arXiv:1203.6409.

[13] D0 collaboration, V. M. Abazov *et al.*, *Measurement of the direct CP-violating charge asymmetry in $D_s^\pm \to \phi\pi^\pm$ decays*, Phys. Rev. Lett. **112** (2014) 111804, arXiv:1312.0741.

[14] LHCb collaboration, A. A. Alves Jr. *et al.*, *The LHCb detector at the LHC*, JINST **3** (2008) S08005.

[15] LHCb collaboration, R. Aaij *et al.*, *LHCb detector performance*, Int. J. Mod. Phys. **A30** (2015) 1530022, arXiv:1412.6352.

[16] T. Sjöstrand, S. Mrenna, and P. Skands, *PYTHIA 6.4 physics and manual*, JHEP **05** (2006) 026, arXiv:hep-ph/0603175.

[17] I. Belyaev *et al.*, *Handling of the generation of primary events in Gauss, the LHCb simulation framework*, J. Phys. Conf. Ser. **331** (2011) 032047.

[18] D. J. Lange, *The EvtGen particle decay simulation package*, Nucl. Instrum. Meth. **A462** (2001) 152.

[19] P. Golonka and Z. Was, *PHOTOS Monte Carlo: A precision tool for QED corrections in Z and W decays*, Eur. Phys. J. **C45** (2006) 97, arXiv:hep-ph/0506026.

[20] Geant4 collaboration, J. Allison *et al.*, *Geant4 developments and applications*, IEEE Trans. Nucl. Sci. **53** (2006) 270; Geant4 collaboration, S. Agostinelli *et al.*, *Geant4: A simulation toolkit*, Nucl. Instrum. Meth. **A506** (2003) 250.

[21] M. Clemencic *et al.*, *The LHCb simulation application, Gauss: Design, evolution and experience*, J. Phys. Conf. Ser. **331** (2011) 032023.

[22] Particle Data Group, C. Patrignani *et al.*, *Review of particle physics*, Chin. Phys. **C40** (2016) 100001.

[23] LHCb collaboration, R. Aaij *et al.*, *Evidence for CP violation in time-integrated $D^0 \to h^- h^+$ decay rates*, Phys. Rev. Lett. **108** (2012) 111602, arXiv:1112.0938.

[24] W. D. Hulsbergen, *Decay chain fitting with a Kalman filter*, Nucl. Instrum. Meth. **A552** (2005) 566, arXiv:physics/0503191.

[25] N. L. Johnson, *Systems of frequency curves generated by methods of translation*, Biometrika **36** (1949) 149.

[26] BaBar collaboration, P. del Amo Sanchez *et al.*, *Study of $B \to X\gamma$ decays and determination of $|V_{td}/V_{ts}|$*, Phys. Rev. **D82** (2010) 051101, arXiv:1005.4087.

[27] LHCb collaboration, R. Aaij *et al.*, *Prompt charm production in pp collisions at $\sqrt{s} = 7$ TeV* , Nucl. Phys. **B871** (2013) 1, arXiv:1302.2864.

[28] LHCb collaboration, R. Aaij *et al.*, *Measurement of $\sigma(pp \to b\bar{b}X)$ at $\sqrt{s} = 7$ TeV in the forward region*, Phys. Lett. **B694** (2010) 209, arXiv:1009.2731.

[29] LHCb collaboration, R. Aaij *et al.*, *Measurements of the branching fractions and CP asymmetries of $B^\pm \to J/\psi\pi^\pm$ and $B^\pm \to \psi(2S)\pi^\pm$ decays*, Phys. Rev. **D85** (2012) 091105(R), arXiv:1203.3592.

[30] LHCb collaboration, R. Aaij *et al.*, *Measurement of CP asymmetries in the decays $B^0 \to K^{*0}\mu^+\mu^-$ and $B^+ \to K^+\mu^+\mu^-$*, JHEP **09** (2014) 177, arXiv:1408.0978.

[31] LHCb collaboration, R. Aaij *et al.*, *Measurement of the $\overline{B}^0$–B^0 and $\overline{B}^0_s$–B^0_s production asymmetries in pp collisions at $\sqrt{s} = 7$ TeV* , Phys. Lett. **B739** (2014) 218, arXiv:1408.0275.

[32] LHCb collaboration, R. Aaij *et al.*, *Measurement of the semileptonic CP asymmetry in B^0–$\overline{B}^0$ mixing*, Phys. Rev. Lett. **114** (2015) 041601, arXiv:1409.8586.

[33] LHCb collaboration, R. Aaij *et al.*, *Observation of the $\Lambda_b^0 \to J/\psi p\pi^-$ decay*, JHEP **07** (2014) 103, arXiv:1406.0755.

[34] ARGUS collaboration, H. Albrecht *et al.*, *Search for hadronic $b \to u$ decays*, Phys. Lett. **B241** (1990) 278.

[35] H.-Y. Cheng and C.-W. Chiang, *Two-body hadronic charmed meson decays*, Phys. Rev. **D81** (2010) 074021, arXiv:1001.0987.

[36] H.-Y. Cheng and C.-W. Chiang, *Direct CP violation in two-body hadronic charmed meson decays*, Phys. Rev. **D85** (2012) 034036, Erratum ibid. **D85** (2012) 079903, arXiv:1201.0785.

[37] H.-n. Li, C.-D. Lu, and F.-S. Yu, *Branching ratios and direct CP asymmetries in $D \to PP$ decays*, Phys. Rev. **D86** (2012) 036012, arXiv:1203.3120.

LHCb collaboration

R. Aaij[40], B. Adeva[39], M. Adinolfi[48], Z. Ajaltouni[5], S. Akar[6], J. Albrecht[10], F. Alessio[40], M. Alexander[53], S. Ali[43], G. Alkhazov[31], P. Alvarez Cartelle[55], A.A. Alves Jr[59], S. Amato[2], S. Amerio[23], Y. Amhis[7], L. An[41], L. Anderlini[18], G. Andreassi[41], M. Andreotti[17,g], J.E. Andrews[60], R.B. Appleby[56], F. Archilli[43], P. d'Argent[12], J. Arnau Romeu[6], A. Artamonov[37], M. Artuso[61], E. Aslanides[6], G. Auriemma[26], M. Baalouch[5], I. Babuschkin[56], S. Bachmann[12], J.J. Back[50], A. Badalov[38], C. Baesso[62], S. Baker[55], W. Baldini[17], R.J. Barlow[56], C. Barschel[40], S. Barsuk[7], W. Barter[40], M. Baszczyk[27], V. Batozskaya[29], B. Batsukh[61], V. Battista[41], A. Bay[41], L. Beaucourt[4], J. Beddow[53], F. Bedeschi[24], I. Bediaga[1], L.J. Bel[43], V. Bellee[41], N. Belloli[21,i], K. Belous[37], I. Belyaev[32], E. Ben-Haim[8], G. Bencivenni[19], S. Benson[43], J. Benton[48], A. Berezhnoy[33], R. Bernet[42], A. Bertolin[23], C. Betancourt[42], F. Betti[15], M.-O. Bettler[40], M. van Beuzekom[43], Ia. Bezshyiko[42], S. Bifani[47], P. Billoir[8], T. Bird[56], A. Birnkraut[10], A. Bitadze[56], A. Bizzeti[18,u], T. Blake[50], F. Blanc[41], J. Blouw[11,†], S. Blusk[61], V. Bocci[26], T. Boettcher[58], A. Bondar[36,w], N. Bondar[31,40], W. Bonivento[16], I. Bordyuzhin[32], A. Borgheresi[21,i], S. Borghi[56], M. Borisyak[35], M. Borsato[39], F. Bossu[7], M. Boubdir[9], T.J.V. Bowcock[54], E. Bowen[42], C. Bozzi[17,40], S. Braun[12], M. Britsch[12], T. Britton[61], J. Brodzicka[56], E. Buchanan[48], C. Burr[56], A. Bursche[2], J. Buytaert[40], S. Cadeddu[16], R. Calabrese[17,g], M. Calvi[21,i], M. Calvo Gomez[38,m], A. Camboni[38], P. Campana[19], D.H. Campora Perez[40], L. Capriotti[56], A. Carbone[15,e], G. Carboni[25,j], R. Cardinale[20,h], A. Cardini[16], P. Carniti[21,i], L. Carson[52], K. Carvalho Akiba[2], G. Casse[54], L. Cassina[21,i], L. Castillo Garcia[41], M. Cattaneo[40], Ch. Cauet[10], G. Cavallero[20], R. Cenci[24,t], D. Chamont[7], M. Charles[8], Ph. Charpentier[40], G. Chatzikonstantinidis[47], M. Chefdeville[4], S. Chen[56], S.-F. Cheung[57], V. Chobanova[39], M. Chrzaszcz[42,27], X. Cid Vidal[39], G. Ciezarek[43], P.E.L. Clarke[52], M. Clemencic[40], H.V. Cliff[49], J. Closier[40], V. Coco[59], J. Cogan[6], E. Cogneras[5], V. Cogoni[16,40,f], L. Cojocariu[30], G. Collazuol[23,o], P. Collins[40], A. Comerma-Montells[12], A. Contu[40], A. Cook[48], G. Coombs[40], S. Coquereau[38], G. Corti[40], M. Corvo[17,g], C.M. Costa Sobral[50], B. Couturier[40], G.A. Cowan[52], D.C. Craik[52], A. Crocombe[50], M. Cruz Torres[62], S. Cunliffe[55], R. Currie[55], C. D'Ambrosio[40], F. Da Cunha Marinho[2], E. Dall'Occo[43], J. Dalseno[48], P.N.Y. David[43], A. Davis[59], O. De Aguiar Francisco[2], K. De Bruyn[6], S. De Capua[56], M. De Cian[12], J.M. De Miranda[1], L. De Paula[2], M. De Serio[14,d], P. De Simone[19], C.T. Dean[53], D. Decamp[4], M. Deckenhoff[10], L. Del Buono[8], M. Demmer[10], A. Dendek[28], D. Derkach[35], O. Deschamps[5], F. Dettori[40], B. Dey[22], A. Di Canto[40], H. Dijkstra[40], F. Dordei[40], M. Dorigo[41], A. Dosil Suárez[39], A. Dovbnya[45], K. Dreimanis[54], L. Dufour[43], G. Dujany[56], K. Dungs[40], P. Durante[40], R. Dzhelyadin[37], A. Dziurda[40], A. Dzyuba[31], N. Déléage[4], S. Easo[51], M. Ebert[52], U. Egede[55], V. Egorychev[32], S. Eidelman[36,w], S. Eisenhardt[52], U. Eitschberger[10], R. Ekelhof[10], L. Eklund[53], S. Ely[61], S. Esen[12], H.M. Evans[49], T. Evans[57], A. Falabella[15], N. Farley[47], S. Farry[54], R. Fay[54], D. Fazzini[21,i], D. Ferguson[52], A. Fernandez Prieto[39], F. Ferrari[15,40], F. Ferreira Rodrigues[2], M. Ferro-Luzzi[40], S. Filippov[34], R.A. Fini[14], M. Fiore[17,g], M. Fiorini[17,g], M. Firlej[28], C. Fitzpatrick[41], T. Fiutowski[28], F. Fleuret[7,b], K. Fohl[40], M. Fontana[16,40], F. Fontanelli[20,h], D.C. Forshaw[61], R. Forty[40], V. Franco Lima[54], M. Frank[40], C. Frei[40], J. Fu[22,q], E. Furfaro[25,j], C. Färber[40], A. Gallas Torreira[39], D. Galli[15,e], S. Gallorini[23], S. Gambetta[52], M. Gandelman[2], P. Gandini[57], Y. Gao[3], L.M. Garcia Martin[69], J. García Pardiñas[39], J. Garra Tico[49], L. Garrido[38], P.J. Garsed[49], D. Gascon[38], C. Gaspar[40], L. Gavardi[10], G. Gazzoni[5], D. Gerick[12], E. Gersabeck[12], M. Gersabeck[56], T. Gershon[50], Ph. Ghez[4], S. Gianì[41], V. Gibson[49], O.G. Girard[41], L. Giubega[30], K. Gizdov[52], V.V. Gligorov[8], D. Golubkov[32], A. Golutvin[55,40], A. Gomes[1,a], I.V. Gorelov[33], C. Gotti[21,i], M. Grabalosa Gándara[5], R. Graciani Diaz[38], L.A. Granado Cardoso[40], E. Graugés[38], E. Graverini[42], G. Graziani[18], A. Grecu[30], P. Griffith[47], L. Grillo[21,40,i], B.R. Gruberg Cazon[57], O. Grünberg[67], E. Gushchin[34], Yu. Guz[37], T. Gys[40],

C. Göbel[62], T. Hadavizadeh[57], C. Hadjivasiliou[5], G. Haefeli[41], C. Haen[40], S.C. Haines[49], S. Hall[55], B. Hamilton[60], X. Han[12], S. Hansmann-Menzemer[12], N. Harnew[57], S.T. Harnew[48], J. Harrison[56], M. Hatch[40], J. He[63], T. Head[41], A. Heister[9], K. Hennessy[54], P. Henrard[5], L. Henry[8], J.A. Hernando Morata[39], E. van Herwijnen[40], M. Heß[67], A. Hicheur[2], D. Hill[57], C. Hombach[56], H. Hopchev[41], W. Hulsbergen[43], T. Humair[55], M. Hushchyn[35], N. Hussain[57], D. Hutchcroft[54], M. Idzik[28], P. Ilten[58], R. Jacobsson[40], A. Jaeger[12], J. Jalocha[57], E. Jans[43], A. Jawahery[60], F. Jiang[3], M. John[57], D. Johnson[40], C.R. Jones[49], C. Joram[40], B. Jost[40], N. Jurik[61], S. Kandybei[45], W. Kanso[6], M. Karacson[40], J.M. Kariuki[48], S. Karodia[53], M. Kecke[12], M. Kelsey[61], I.R. Kenyon[47], M. Kenzie[49], T. Ketel[44], E. Khairullin[35], B. Khanji[12], C. Khurewathanakul[41], T. Kirn[9], S. Klaver[56], K. Klimaszewski[29], S. Koliiev[46], M. Kolpin[12], I. Komarov[41], R.F. Koopman[44], P. Koppenburg[43], A. Kosmyntseva[32], A. Kozachuk[33], M. Kozeiha[5], L. Kravchuk[34], K. Kreplin[12], M. Kreps[50], P. Krokovny[36,w], F. Kruse[10], W. Krzemien[29], W. Kucewicz[27,l], M. Kucharczyk[27], V. Kudryavtsev[36,w], A.K. Kuonen[41], K. Kurek[29], T. Kvaratskheliya[32,40], D. Lacarrere[40], G. Lafferty[56], A. Lai[16], G. Lanfranchi[19], C. Langenbruch[9], T. Latham[50], C. Lazzeroni[47], R. Le Gac[6], J. van Leerdam[43], J.-P. Lees[4], A. Leflat[33,40], J. Lefrançois[7], R. Lefèvre[5], F. Lemaitre[40], E. Lemos Cid[39], O. Leroy[6], T. Lesiak[27], B. Leverington[12], Y. Li[7], T. Likhomanenko[35,68], R. Lindner[40], C. Linn[40], F. Lionetto[42], B. Liu[16], X. Liu[3], D. Loh[50], I. Longstaff[53], J.H. Lopes[2], D. Lucchesi[23,o], M. Lucio Martinez[39], H. Luo[52], A. Lupato[23], E. Luppi[17,g], O. Lupton[57], A. Lusiani[24], X. Lyu[63], F. Machefert[7], F. Maciuc[30], O. Maev[31], K. Maguire[56], S. Malde[57], A. Malinin[68], T. Maltsev[36], G. Manca[7], G. Mancinelli[6], P. Manning[61], J. Maratas[5,v], J.F. Marchand[4], U. Marconi[15], C. Marin Benito[38], P. Marino[24,t], J. Marks[12], G. Martellotti[26], M. Martin[6], M. Martinelli[41], D. Martinez Santos[39], F. Martinez Vidal[69], D. Martins Tostes[2], L.M. Massacrier[7], A. Massafferri[1], R. Matev[40], A. Mathad[50], Z. Mathe[40], C. Matteuzzi[21], A. Mauri[42], B. Maurin[41], A. Mazurov[47], M. McCann[55], J. McCarthy[47], A. McNab[56], R. McNulty[13], B. Meadows[59], F. Meier[10], M. Meissner[12], D. Melnychuk[29], M. Merk[43], A. Merli[22,q], E. Michielin[23], D.A. Milanes[66], M.-N. Minard[4], D.S. Mitzel[12], M.P. Mocci[24,p], A. Mogini[8], J. Molina Rodriguez[1], I.A. Monroy[66], S. Monteil[5], M. Morandin[23], P. Morawski[28], A. Mordà[6], M.J. Morello[24,t], J. Moron[28], A.B. Morris[52], R. Mountain[61], F. Muheim[52], M. Mulder[43], M. Mussini[15], D. Müller[56], J. Müller[10], K. Müller[42], V. Müller[10], P. Naik[48], T. Nakada[41], R. Nandakumar[51], A. Nandi[57], I. Nasteva[2], M. Needham[52], N. Neri[22], S. Neubert[12], N. Neufeld[40], M. Neuner[12], A.D. Nguyen[41], T.D. Nguyen[41], C. Nguyen-Mau[41,n], S. Nieswand[9], R. Niet[10], N. Nikitin[33], T. Nikodem[12], A. Novoselov[37], D.P. O'Hanlon[50], A. Oblakowska-Mucha[28], V. Obraztsov[37], S. Ogilvy[19], R. Oldeman[49], C.J.G. Onderwater[70], J.M. Otalora Goicochea[2], A. Otto[40], P. Owen[42], A. Oyanguren[69,40], P.R. Pais[41], A. Palano[14,d], F. Palombo[22,q], M. Palutan[19], J. Panman[40], A. Papanestis[51], M. Pappagallo[14,d], L.L. Pappalardo[17,g], W. Parker[60], C. Parkes[56], G. Passaleva[18], A. Pastore[14,d], G.D. Patel[54], M. Patel[55], C. Patrignani[15,e], A. Pearce[56,51], A. Pellegrino[43], G. Penso[26], M. Pepe Altarelli[40], S. Perazzini[40], P. Perret[5], L. Pescatore[47], K. Petridis[48], A. Petrolini[20,h], A. Petrov[68], M. Petruzzo[22,q], E. Picatoste Olloqui[38], B. Pietrzyk[4], M. Pikies[27], D. Pinci[26], A. Pistone[20], A. Piucci[12], S. Playfer[52], M. Plo Casasus[39], T. Poikela[40], F. Polci[8], A. Poluektov[50,36], I. Polyakov[61], E. Polycarpo[2], G.J. Pomery[48], A. Popov[37], D. Popov[11,40], B. Popovici[30], S. Poslavskii[37], C. Potterat[2], E. Price[48], J.D. Price[54], J. Prisciandaro[39], A. Pritchard[54], C. Prouve[48], V. Pugatch[46], A. Puig Navarro[41], G. Punzi[24,p], W. Qian[57], R. Quagliani[7,48], B. Rachwal[27], J.H. Rademacker[48], M. Rama[24], M. Ramos Pernas[39], M.S. Rangel[2], I. Raniuk[45], F. Ratnikov[35], G. Raven[44], F. Redi[55], S. Reichert[10], A.C. dos Reis[1], C. Remon Alepuz[69], V. Renaudin[7], S. Ricciardi[51], S. Richards[48], M. Rihl[40], K. Rinnert[54], V. Rives Molina[38], P. Robbe[7,40], A.B. Rodrigues[1], E. Rodrigues[59], J.A. Rodriguez Lopez[66], P. Rodriguez Perez[56,†], A. Rogozhnikov[35], S. Roiser[40], A. Rollings[57], V. Romanovskiy[37], A. Romero Vidal[39], J.W. Ronayne[13], M. Rotondo[19], M.S. Rudolph[61], T. Ruf[40], P. Ruiz Valls[69], J.J. Saborido Silva[39], E. Sadykhov[32], N. Sagidova[31], B. Saitta[16,f],

V. Salustino Guimaraes[2], C. Sanchez Mayordomo[69], B. Sanmartin Sedes[39], R. Santacesaria[26], C. Santamarina Rios[39], M. Santimaria[19], E. Santovetti[25,j], A. Sarti[19,k], C. Satriano[26,s], A. Satta[25], D.M. Saunders[48], D. Savrina[32,33], S. Schael[9], M. Schellenberg[10], M. Schiller[40], H. Schindler[40], M. Schlupp[10], M. Schmelling[11], T. Schmelzer[10], B. Schmidt[40], O. Schneider[41], A. Schopper[40], K. Schubert[10], M. Schubiger[41], M.-H. Schune[7], R. Schwemmer[40], B. Sciascia[19], A. Sciubba[26,k], A. Semennikov[32], A. Sergi[47], N. Serra[42], J. Serrano[6], L. Sestini[23], P. Seyfert[21], M. Shapkin[37], I. Shapoval[45], Y. Shcheglov[31], T. Shears[54], L. Shekhtman[36,w], V. Shevchenko[68], B.G. Siddi[17,40], R. Silva Coutinho[42], L. Silva de Oliveira[2], G. Simi[23,o], S. Simone[14,d], M. Sirendi[49], N. Skidmore[48], T. Skwarnicki[61], E. Smith[55], I.T. Smith[52], J. Smith[49], M. Smith[55], H. Snoek[43], M.D. Sokoloff[59], F.J.P. Soler[53], B. Souza De Paula[2], B. Spaan[10], P. Spradlin[53], S. Sridharan[40], F. Stagni[40], M. Stahl[12], S. Stahl[40], P. Stefko[41], S. Stefkova[55], O. Steinkamp[42], S. Stemmle[12], O. Stenyakin[37], S. Stevenson[57], S. Stoica[30], S. Stone[61], B. Storaci[42], S. Stracka[24,p], M. Straticiuc[30], U. Straumann[42], L. Sun[64], W. Sutcliffe[55], K. Swientek[28], V. Syropoulos[44], M. Szczekowski[29], T. Szumlak[28], S. T'Jampens[4], A. Tayduganov[6], T. Tekampe[10], M. Teklishyn[7], G. Tellarini[17,g], F. Teubert[40], E. Thomas[40], J. van Tilburg[43], M.J. Tilley[55], V. Tisserand[4], M. Tobin[41], S. Tolk[49], L. Tomassetti[17,g], D. Tonelli[40], S. Topp-Joergensen[57], F. Toriello[61], E. Tournefier[4], S. Tourneur[41], K. Trabelsi[41], M. Traill[53], M.T. Tran[41], M. Tresch[42], A. Trisovic[40], A. Tsaregorodtsev[6], P. Tsopelas[43], A. Tully[49], N. Tuning[43], A. Ukleja[29], A. Ustyuzhanin[35], U. Uwer[12], C. Vacca[16,f], V. Vagnoni[15,40], A. Valassi[40], S. Valat[40], G. Valenti[15], A. Vallier[7], R. Vazquez Gomez[19], P. Vazquez Regueiro[39], S. Vecchi[17], M. van Veghel[43], J.J. Velthuis[48], M. Veltri[18,r], G. Veneziano[57], A. Venkateswaran[61], M. Vernet[5], M. Vesterinen[12], B. Viaud[7], D. Vieira[1], M. Vieites Diaz[39], H. Viemann[67], X. Vilasis-Cardona[38,m], M. Vitti[49], V. Volkov[33], A. Vollhardt[42], B. Voneki[40], A. Vorobyev[31], V. Vorobyev[36,w], C. Voß[67], J.A. de Vries[43], C. Vázquez Sierra[39], R. Waldi[67], C. Wallace[50], R. Wallace[13], J. Walsh[24], J. Wang[61], D.R. Ward[49], H.M. Wark[54], N.K. Watson[47], D. Websdale[55], A. Weiden[42], M. Whitehead[40], J. Wicht[50], G. Wilkinson[57,40], M. Wilkinson[61], M. Williams[40], M.P. Williams[47], M. Williams[58], T. Williams[47], F.F. Wilson[51], J. Wimberley[60], J. Wishahi[10], W. Wislicki[29], M. Witek[27], G. Wormser[7], S.A. Wotton[49], K. Wraight[53], K. Wyllie[40], Y. Xie[65], Z. Xing[61], Z. Xu[41], Z. Yang[3], Y. Yao[61], H. Yin[65], J. Yu[65], X. Yuan[36,w], O. Yushchenko[37], K.A. Zarebski[47], M. Zavertyaev[11,c], L. Zhang[3], Y. Zhang[7], Y. Zhang[63], A. Zhelezov[12], Y. Zheng[63], A. Zhokhov[32], X. Zhu[3], V. Zhukov[9], S. Zucchelli[15].

[1] *Centro Brasileiro de Pesquisas Físicas (CBPF), Rio de Janeiro, Brazil*
[2] *Universidade Federal do Rio de Janeiro (UFRJ), Rio de Janeiro, Brazil*
[3] *Center for High Energy Physics, Tsinghua University, Beijing, China*
[4] *LAPP, Université Savoie Mont-Blanc, CNRS/IN2P3, Annecy-Le-Vieux, France*
[5] *Clermont Université, Université Blaise Pascal, CNRS/IN2P3, LPC, Clermont-Ferrand, France*
[6] *CPPM, Aix-Marseille Université, CNRS/IN2P3, Marseille, France*
[7] *LAL, Université Paris-Sud, CNRS/IN2P3, Orsay, France*
[8] *LPNHE, Université Pierre et Marie Curie, Université Paris Diderot, CNRS/IN2P3, Paris, France*
[9] *I. Physikalisches Institut, RWTH Aachen University, Aachen, Germany*
[10] *Fakultät Physik, Technische Universität Dortmund, Dortmund, Germany*
[11] *Max-Planck-Institut für Kernphysik (MPIK), Heidelberg, Germany*
[12] *Physikalisches Institut, Ruprecht-Karls-Universität Heidelberg, Heidelberg, Germany*
[13] *School of Physics, University College Dublin, Dublin, Ireland*
[14] *Sezione INFN di Bari, Bari, Italy*
[15] *Sezione INFN di Bologna, Bologna, Italy*
[16] *Sezione INFN di Cagliari, Cagliari, Italy*
[17] *Sezione INFN di Ferrara, Ferrara, Italy*
[18] *Sezione INFN di Firenze, Firenze, Italy*
[19] *Laboratori Nazionali dell'INFN di Frascati, Frascati, Italy*
[20] *Sezione INFN di Genova, Genova, Italy*
[21] *Sezione INFN di Milano Bicocca, Milano, Italy*

[22] *Sezione INFN di Milano, Milano, Italy*
[23] *Sezione INFN di Padova, Padova, Italy*
[24] *Sezione INFN di Pisa, Pisa, Italy*
[25] *Sezione INFN di Roma Tor Vergata, Roma, Italy*
[26] *Sezione INFN di Roma La Sapienza, Roma, Italy*
[27] *Henryk Niewodniczanski Institute of Nuclear Physics Polish Academy of Sciences, Kraków, Poland*
[28] *AGH - University of Science and Technology, Faculty of Physics and Applied Computer Science, Kraków, Poland*
[29] *National Center for Nuclear Research (NCBJ), Warsaw, Poland*
[30] *Horia Hulubei National Institute of Physics and Nuclear Engineering, Bucharest-Magurele, Romania*
[31] *Petersburg Nuclear Physics Institute (PNPI), Gatchina, Russia*
[32] *Institute of Theoretical and Experimental Physics (ITEP), Moscow, Russia*
[33] *Institute of Nuclear Physics, Moscow State University (SINP MSU), Moscow, Russia*
[34] *Institute for Nuclear Research of the Russian Academy of Sciences (INR RAN), Moscow, Russia*
[35] *Yandex School of Data Analysis, Moscow, Russia*
[36] *Budker Institute of Nuclear Physics (SB RAS), Novosibirsk, Russia*
[37] *Institute for High Energy Physics (IHEP), Protvino, Russia*
[38] *ICCUB, Universitat de Barcelona, Barcelona, Spain*
[39] *Universidad de Santiago de Compostela, Santiago de Compostela, Spain*
[40] *European Organization for Nuclear Research (CERN), Geneva, Switzerland*
[41] *Institute of Physics, Ecole Polytechnique Fédérale de Lausanne (EPFL), Lausanne, Switzerland*
[42] *Physik-Institut, Universität Zürich, Zürich, Switzerland*
[43] *Nikhef National Institute for Subatomic Physics, Amsterdam, The Netherlands*
[44] *Nikhef National Institute for Subatomic Physics and VU University Amsterdam, Amsterdam, The Netherlands*
[45] *NSC Kharkiv Institute of Physics and Technology (NSC KIPT), Kharkiv, Ukraine*
[46] *Institute for Nuclear Research of the National Academy of Sciences (KINR), Kyiv, Ukraine*
[47] *University of Birmingham, Birmingham, United Kingdom*
[48] *H.H. Wills Physics Laboratory, University of Bristol, Bristol, United Kingdom*
[49] *Cavendish Laboratory, University of Cambridge, Cambridge, United Kingdom*
[50] *Department of Physics, University of Warwick, Coventry, United Kingdom*
[51] *STFC Rutherford Appleton Laboratory, Didcot, United Kingdom*
[52] *School of Physics and Astronomy, University of Edinburgh, Edinburgh, United Kingdom*
[53] *School of Physics and Astronomy, University of Glasgow, Glasgow, United Kingdom*
[54] *Oliver Lodge Laboratory, University of Liverpool, Liverpool, United Kingdom*
[55] *Imperial College London, London, United Kingdom*
[56] *School of Physics and Astronomy, University of Manchester, Manchester, United Kingdom*
[57] *Department of Physics, University of Oxford, Oxford, United Kingdom*
[58] *Massachusetts Institute of Technology, Cambridge, MA, United States*
[59] *University of Cincinnati, Cincinnati, OH, United States*
[60] *University of Maryland, College Park, MD, United States*
[61] *Syracuse University, Syracuse, NY, United States*
[62] *Pontifícia Universidade Católica do Rio de Janeiro (PUC-Rio), Rio de Janeiro, Brazil, associated to* [2]
[63] *University of Chinese Academy of Sciences, Beijing, China, associated to* [3]
[64] *School of Physics and Technology, Wuhan University, Wuhan, China, associated to* [3]
[65] *Institute of Particle Physics, Central China Normal University, Wuhan, Hubei, China, associated to* [3]
[66] *Departamento de Fisica , Universidad Nacional de Colombia, Bogota, Colombia, associated to* [8]
[67] *Institut für Physik, Universität Rostock, Rostock, Germany, associated to* [12]
[68] *National Research Centre Kurchatov Institute, Moscow, Russia, associated to* [32]
[69] *Instituto de Fisica Corpuscular, Centro Mixto Universidad de Valencia - CSIC, Valencia, Spain, associated to* [38]
[70] *Van Swinderen Institute, University of Groningen, Groningen, The Netherlands, associated to* [43]

[a] *Universidade Federal do Triângulo Mineiro (UFTM), Uberaba-MG, Brazil*
[b] *Laboratoire Leprince-Ringuet, Palaiseau, France*
[c] *P.N. Lebedev Physical Institute, Russian Academy of Science (LPI RAS), Moscow, Russia*
[d] *Università di Bari, Bari, Italy*

[e] *Università di Bologna, Bologna, Italy*
[f] *Università di Cagliari, Cagliari, Italy*
[g] *Università di Ferrara, Ferrara, Italy*
[h] *Università di Genova, Genova, Italy*
[i] *Università di Milano Bicocca, Milano, Italy*
[j] *Università di Roma Tor Vergata, Roma, Italy*
[k] *Università di Roma La Sapienza, Roma, Italy*
[l] *AGH - University of Science and Technology, Faculty of Computer Science, Electronics and Telecommunications, Kraków, Poland*
[m] *LIFAELS, La Salle, Universitat Ramon Llull, Barcelona, Spain*
[n] *Hanoi University of Science, Hanoi, Viet Nam*
[o] *Università di Padova, Padova, Italy*
[p] *Università di Pisa, Pisa, Italy*
[q] *Università degli Studi di Milano, Milano, Italy*
[r] *Università di Urbino, Urbino, Italy*
[s] *Università della Basilicata, Potenza, Italy*
[t] *Scuola Normale Superiore, Pisa, Italy*
[u] *Università di Modena e Reggio Emilia, Modena, Italy*
[v] *Iligan Institute of Technology (IIT), Iligan, Philippines*
[w] *Novosibirsk State University, Novosibirsk, Russia*

[†] *Deceased*